Received: 16 March 2020 | Revised: 30 March 2020 | Accepted: 1 April 2020

DOI: 10.1002/pol.20200172

ORIGINAL ARTICLE

JOURNAL OF POLYMER SCIENCE WILEY

Synthesis and characterization of hydrogels containing redox-responsive 2,2,6,6-tetramethylpiperidinyloxy methacrylate and thermoresponsive *N*-isopropylacrylamide

Miriam Khodeir[1] | He Jia[1] | Sayed Antoun[2] | Christian Friebe[3] | Ulrich S. Schubert[3] | Yan Lu[4,5] | Evelyne Van Ruymbeke[1] | Jean-François Gohy[1]

[1]Institute of Condensed Matter and Nanosciences (IMCN), Bio and Soft Matter (BSMA), Université Catholique de Louvain (UCL), Louvain-la-Neuve, Belgium

[2]Department of Chemistry, Faculty of Science Section III - North Campus-Tripoli, Lebanese University (UL), Lebanon

[3]Laboratory of Organic and Macromolecular Chemistry (IOMC), Friedrich Schiller Universität Jena, Jena, Germany

[4]EM-IEES Institute for Electrochemical Energy Storage, Helmholtz-Zentrum Berlin für Materialien und Energie, Berlin, Germany

[5]Institute of Chemistry, University of Potsdam, Potsdam, Germany

Correspondence
Jean-François Gohy, Institute of Condensed Matter and Nanosciences (IMCN), Bio and Soft Matter (BSMA), Université Catholique de Louvain (UCL), Place L. Pasteur 1 & Croix du Sud 1, B-1348 Louvain-la-Neuve, Belgium.
Email: jean-francois.gohy@uclouvain.be

Funding information
RIS3 Innovation Center CEEC Jena; Fondation Louvain; Concerted Research Action BATTAB, Grant/Award Number: 14/19-057; International Relations Office (ADRI) of UClouvain

Abstract

Smart hydrogels containing 2,2,6,6-tetramethylpiperidinoxy methacrylate (TEMPO) and *N*-isopropylacrylamide (NIPAM) that undergo reversible redox behavior are prepared and investigated. Several polymer networks are first prepared by free-radical copolymerization of varying amounts of TEMPO, NIPAM, and a crosslinker (diethylene glycol diacrylate) and subsequently swelled with water to lead to hydrogels. In order to investigate the effects of the redox activity of TEMPO units and of the lower critical solution temperature of NIPAM on the hydrogel properties, a study of the swelling ratio of the polymer networks in distilled water at different temperatures is performed for the two forms of TEMPO, the reduced (TEMPO) and oxidized ($TEMPO^+$) one. Moreover, the rheological properties are also measured for both hydrogel forms. Finally, the encapsulation abilities of the oxidized hydrogels are demonstrated via electrostatic interactions between positively charged $TEMPO^+$ units and negatively charged guest molecules, supporting future application of our system in the biomedical and environmental fields.

KEYWORDS

hydrogels, NIPAM, redox, stimuli-responsive, TEMPO

1 | INTRODUCTION

In the last few decades, the focus on the so-called "smart" materials has grown enormously. Stimuli-responsive materials are examples of these developments,[1] which possess the ability to respond to external stimuli such as temperature,[2] pH,[3] humidity,[4] light,[5] specific ions or molecules,[6] electrical fields,[7] solvent and ionic strength,[8] and so forth. Polymers represent attractive candidates for smart materials because they may contain different domains or moieties, each of them with specific properties that may lead to multiresponsive systems. Moreover, polymers can form extended three-dimensional structures which hold the solvent. Hydrogels are typical examples of such structures in which a crosslinked three-dimensional network of polymer holds water without dissolution. Depending on the monomers incorporated into the hydrogel and the conditions of the surrounding medium, hydrogels can exhibit a full range of properties. As a typical example, the work of Singh et al. showed that the swelling properties of poly(*N*-isopropylacrylamide) (PNIPAM) containing hydrogels could be tailored by incorporating various contents of poly(ethylene glycol) methacrylate (PEGMA) as well as by the conditions of polymerization.[9] In this respect, the lower critical solution temperature (LCST) of PNIPAM was increased by increasing amount of PEGMA and was attaining a temperature of 37°C after copolymerization with 10 wt% of PEGMA. Moreover, the copolymer composition also had a large effect on the cell growth and detachment.[9]

As already highlighted in the example before, hydrogels as biocompatible materials[10] are quite promising for applications in aqueous media.[11] And they become in particular useful when they are used as "smart" materials.[11] As far as aqueous media are concerned, temperature and pH value changes are the most commonly studied stimuli since these parameters can be easily controlled. Thermoresponsive hydrogels have been recently increasingly investigated and are usually prepared from thermosensitive polymers with an LCST.[12] More precisely, around the critical temperature, the polymer in aqueous solution exhibits a phase transition from a soluble to an insoluble state. Among the known LCST polymers, PNIPAM is one of the most promising because of its LCST (32°C) is close to human body temperature and relatively insensitive to environmental conditions. There are numerous examples referring to PNIPAM hydrogels[13–16] and many applications are in aqueous medium in which they swell to a very high degree.[17–19] This requires a low density of slightly crosslinked PNIPAM chains which makes the gels extremely poor in mechanical strength. This constitutes a great hurdle in their applications.

On the other hand, hydrogels with redox responsiveness have been scarcely reported compared to the other stimuli such as pH value and temperature changes. As typical examples, hydrogels containing disulfide crosslinkers can be cited, in which the redox stimulus is used to break disulfide bonds by reduction into thiol groups resulting in the disruption of the polymer network, the dissolution of the hydrogel and eventually in the release of guest molecules.[20] Another example involves ferrocene groups that can modify the hydrophilic–hydrophobic balance of the hydrogel depending on their redox state.[21] Final examples of redox responsive polymer involve conducting polymers, such as polyaniline or polypyrrole, in which clusters of conductive polymers are entrapped into the hydrogels. When submitted to an electrical current the conductive polymers become hydrophilic and allow the encapsulated drug to diffuse out of the hydrogel.[22] Stable nitroxide radicals like 2,2,6,6-tetramethylpiperidinoxyl (TEMPO) derivatives can be reversibly oxidized or reduced. This process underlies the use of TEMPO as an organic catalyst for oxidations in organic synthesis.[23] This redox process is also widely used for energy storage applications as highlighted by the pioneering work of Hiroyuki and Kenichi to design TEMPO-containing polymers as organic battery materials.[24]

We recently reported the synthesis and characterization of redox hydrogels based on poly(2,-2,6,6-tetramethylpiperidinyloxy methacrylate-*statistical*-oligoethyleneglycol methacrylate) (P[TEMPO-*s*-OEGMA]) copolymer.[25] In these hydrogels, the OEGMA comonomer brings the hydrophilicity to the polymer network, the TEMPO methacrylate component being hydrophobic in its reduced form. Although, OEGMA is characterized by an LCST behavior, its cloud point is located at a too high temperature (above 60°C) to allow the hydrogel to be exploited for bio-applications.[26] This prompted us to replace it by NIPAM, inspired by the work of Fu et al.[27] Therefore, the present contribution aims at synthesizing poly(TEMPO-*statistical*-*N*-isopropylacrylamide) (P[TEMPO-*s*-NIPAM]) copolymer networks and studying the effects of the redox and temperature stimuli on their mechanical and physicochemical properties.

2 | EXPERIMENTAL

2.1 | Materials

All chemicals and monomers were purchased from Aldrich, TCI, or Acros. Solvents were bought from Acros and VWR. NIPAM (Acros) and diethylene glycol

diacrylate (DEGDA, Aldrich) were purified on an AlOx-filtration column prior use in order to remove the inhibitor.

2.2 | Instrumentation

2.2.1 | Proton nuclear magnetic resonance spectroscopy

Proton nuclear magnetic resonance (^{1}H NMR) spectra were acquired on a 300 MHz Bruker Avance II in acetonitrile for the hydrogel obtained after polymerization.

2.2.2 | Ultraviolet–visible spectroscopy

After equilibration of the oxidized hydrogel swollen in Eosin B solution at a concentration of 0.012 g/L, the supernatant was transferred into quartz cuvettes and tested using a Varian Cary 50 UV–vis spectrophotometer with emission scans recorded from 250 to 800 nm.

2.2.3 | Rheological measurements

Rheological experiments were performed on a Kinexus Ultra (Malvern Instruments) rheometer equipped with a heat exchanger and modified with a solvent trap. Measurements were carried out using a plate–plate steel geometry (8 and 20 mm diameters) with a gap adjusted between 450 and 1,800 mm so that the geometry was completely filled. Oscillatory measurements were carried out in the linear regime (either at strain control of 1% or at stress control of 5 Pa). Strain sweep measurements have also been performed at a strain amplitude ranging from 0.3 to 1,000% and at a frequency of 5 rad/s[1]. Measurements were carried out at 20°C in a water saturated atmosphere in order to minimize evaporation of the solvent. Normal forces were checked to be relaxed to ~0.05 N prior to any measurement.

2.2.4 | Swelling tests

The dry gels were swollen in distilled water at 25°C in an isothermal water bath to study the equilibrium swelling kinetics. Mass measurements were taken at time intervals of 0, 0.5, 1, 2, 4, 8, 24, and 48 hr. The swelling factor was defined as the weight ratio between the difference in hydrogel weight in both the dry and the swollen state over the weight of the dry gel. A temperature swelling study was conducted; gels were swelled from 10 to 80°C with increments of 5°C. An equilibration time of 24 hr was used before each measurement and mass swelling ratios at each temperature were calculated.

2.2.5 | Electron spin resonance

The EPR spin count was determined as the mean value achieved from the EPR spectra of three different samples of the same TEMPO-containing gel. For comparison, the EPR spin count of a TEMPO-free gel was determined likewise. X-band EPR spectra were acquired on an EMXmicro CW EPR spectrometer from Bruker, Germany (EMX micro EMM-6/ 1/9-VT control unit, ER 070 magnet, EMX premium ER04 Xband microwave bridge equipped with an EMX standard resonator, EMX080 power unit). The samples were investigated at room temperature and the data handling was done with the Bruker Xenon software package, version 1.1b86. The SpinCountQ software module was used for the determination of the spin count.

2.2.6 | Cryogenic-transmission electron microscopy

For the cryogenic-transmission electron microscopy (cryo-TEM) measurements, a 4 ml droplet of diluted sample suspension was dropped onto lacey carbon copper grids (200 mesh, Science Services) and plunge frozen into liquid ethane using a Vitrobot Mark IV (FEI, Eindhoven, Netherlands), which was set at 4°C with 95% humidity. Vitrified grids were then mounted on a cryo-transfer holder (Gatan 914; Gatan, Munich, Germany) and transferred into a JEOL JEM2100 (JEOL GmbH, Eching, Germany) TEM for imaging with a bottom-mounted 4 × 4k CMOS camera (TemCam-F416; TVIPS, Gauting, Germany). The microscope was operated at an acceleration voltage of 200 kV and a defocus of the objective lens of about 1.5–2 mm was used to increase the contrast. The total electron dose for each micrograph was kept below 20 $e^-/Å^2$.

2.3 | Synthesis

2.3.1 | Typical procedure for the precursor P(TMPM-*s*-NIPAM) network synthesis

The synthesis of the polymer network was carried out using conventional radical polymerization. Into a 50 mL round-bottom flask, TMPM was dissolved in water then

NIPAM and DEGDA crosslinker were added and stirred until a homogeneous blend was achieved. The solution was then degassed by three freeze–pump–thaw cycles. The initiator ammonium persulfate (0.5 eq.) and activator tetramethylethylenediamine (0.5 eq.) were then introduced under argon flux. The solution was immersed in water bath at 25°C and stirred overnight. A transparent gel was formed.

2.3.2 | Typical procedure for the P(TEMPO-*s*-NIPAM) network synthesis

The secondary amine of the TMPM units has been oxidized into a nitroxide radical to lead to TEMPO. For that, water has been evaporated under pressure from the P(TMPM-*s*-NIPAM) hydrogel obtained after polymerization. Then, Na_2WO_4 (0.25 eq.) and EDTA (0.15 eq.) were added and the mixture was swollen in methanol for a couple of hours before adding the oxidizing agent H_2O_2 (5 eq.). The mixture was then stirred at 60°C overnight.[28] An orange colored gel was obtained, washed four times with distilled water and methanol (1:1, vol: vol) and dried in a vacuum at 40°C overnight. An orange sticky material was finally obtained.

2.3.3 | Typical procedure for the oxidized P(TEMPO$^+$-*s*-NIPAM) hydrogel synthesis

The P(TEMPO-*s*-NIPAM) network was swollen in distilled H_2O (31.25 eq.). Then, fluoroboric acid (HBF_4, 1 eq.) was slowly added dropwise over 1 hr at room temperature.[26] Sodium hypochlorite (0.5 eq.) was then added over 1 hr at 0°C and stirred for an additional 1 hr at 0°C to lead to the oxidized P(TEMPO$^+$-*s*-NIPAM) hydrogel. Then, the hydrogel was washed with ice-cold 5 wt% $NaHCO_3$, distilled water, and ice-cold diethyl ether. The obtained yellow gel was finally dried overnight at 40°C in vacuo.

3 | RESULTS AND DISCUSSION

3.1 | Synthesis and characterization of hydrogels

The investigated P(TEMPO$^+$-*s*-NIPAM) hydrogels were synthesized via a three-step methodology as depicted in Figure 1. First, a P(TMPM-*s*-NIPAM) precursor hydrogel was prepared by conventional radical polymerization, followed by the oxidation of the secondary amine of the PTMPM units with H_2O_2 and Na_2WO_4 in methanol to obtain the P(TEMPO-*s*-NIPAM) hydrogel.

Different molar ratios of TMPM/(TMPM + NIPAM + DEGDA) (abbreviated as X_{TEMPO} in the following) were investigated (0.1, 0.2, 0.3, and 0.4) and the crosslinker molar ratio DEGDA/(TMPM + NIPAM + DEGDA) (abbreviated as X_{CL} in the following) was also varied (0.02, 0.03, 0.04, 0.05, and 0.13) to investigate the influence of increasing both TEMPO and DEGDA amounts on the characteristics of the hydrogels.

The yield of the polymerization reaction was checked by ^{1}H NMR by dissolving the dry P(TMPM-*s*-NIPAM) network in $CDCl_3$ and recording a ^{1}H NMR spectrum of the soluble fraction. No signal corresponding to ethylenic protons was detected for all the investigated systems confirming a full conversion of the monomers (Figure S1). Signals corresponding to P(TMPM-*s*-NIPAM) polymer chains were, however, detected in the soluble fraction confirming that the obtained P(TMPM-*s*-NIPAM) networks are slightly crosslinked and that some entrapped P(TMPM-*s*-NIPAM) free chains can be extracted from the hydrogel. The amount of extracted free chains was determined to be 10 ± 1 wt% in agreement with our previously reported results on hydrogels based on OEGMA.[25]

Finally, the nitroxide radical units of TEMPO were oxidized into oxoammonium units (TEMPO$^+$) with NaClO in the presence of HBF_4 to obtain the oxidized P(TEMPO$^+$-*s*-NIPAM) hydrogels. The macroscopic appearance of the synthetized hydrogels is listed in Table 1 in accordance to the X_{TEMPO} and X_{CL} parameters.

The fact that the synthesized P(TEMPO-*s*-NIPAM) networks do not always form hydrogels (Table 1) can be

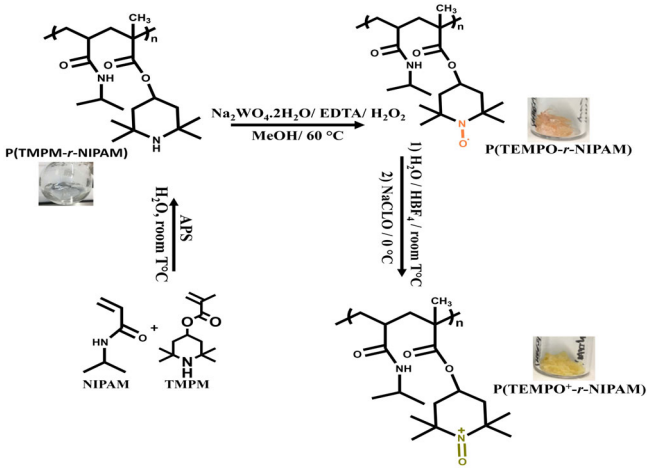

FIGURE 1 Synthesis of poly(2,2,6,6-tetramethylpiperidinoxy methacrylate-*statistical*-*N*-isopropylacrylamide) P(TEMPO$^+$-*s*-NIPAM) hydrogels [Color figure can be viewed at wileyonlinelibrary.com]

explained by different factors. First, with too low concentrations of crosslinking agent (X_{CL} = 0.02, 0.03, and 0.04), it seems that the crosslinking density is too low to allow the formation of a macroscopic hydrogel. Second, the amount of TEMPO (or TMPM before oxidation) in the polymer network is an important parameter driving the formation of a macroscopic hydrogel. Indeed, we have demonstrated in our previous reports that TEMPO (or TMPM before oxidation) units are essentially hydrophobic and aggregate into nanodomains.[25,26] Those hydrophobic interactions are leading to physical crosslinks summing up to the chemical crosslinks provided by the bifunctional DEGDA monomer.

However, since the synthesis of the P(TEMPO-*s*-NIPAM) networks is conducted in aqueous medium, one could consider that the presence of hydrophobic TEMPO hydrophobic nanodomains has little effect on the formation of a macroscopic hydrogel since those nanodomains will be present in all investigated samples. In that respect, the amount of DEGDA crosslinker seems to be the main factor dictating the formation of a macroscopic gel and a value of X_{CL} above 0.05 is needed to observe the systematic formation of hydrogels. This conclusion is corroborated by the expected reactivity ratios (r_1 and r_2) of the TMPM/NIPAM comonomers. Although we have not experimentally determined the reactivity ratios in the present study, it is well known that methacrylate monomers are more reactive than acrylamide ones. As a typical example, Virtanen et al. have determined the reactivity ratios of NIPAM (Monomer 1) and glycidyl methacrylate (Monomer 2) and have found r_1 = 0.39 and r_2 = 2.69.[27] If we assume that a similar situation prevails in our case, we can assume that TMP is consumed first during the copolymerization reaction. Since we are reaching full conversion for the polymerizations carried out in the present study, TEMPO (or TMPM before oxidation) hydrophobic domains do form first during the course of polymerization from which NIPAM-rich blocks are growing in a next step. A significant part of the DEGDA crosslinker could be incorporated into the TEMPO (or TMPM before oxidation) rich domains, explaining why a significant amount of DEGDA is required to observed macroscopic gelation (see Table 1). If this hypothesis is valid, this would mean that kinds of nanogel or micellar structures should be formed during the copolymerization reaction. At the end of the copolymerization reaction, those nanostructures will be eventually connected by chemical crosslinks in order to form the macroscopic hydrogel. In order to validate this hypothesis, we have performed dynamic light scattering (DLS) and cryo-TEM analysis of samples that do not form a macroscopic gel. Indeed, those samples are liquids showing the typical bluish appearance of micellar solutions (Table 1). Figure 2 shows a size distribution analysis obtained by DLS on the P(TEMPO-*s*-NIPAM) sample with and X_{TEMPO} = 0.2 and X_{CL} = 0.03. A single peak corresponding to a mean hydrodynamic radius of 25 nm is observed indicating the presence of micellar nano-objects or nanogel particles.

Figure 3 shows a typical cryo-TEM picture for the same P(TEMPO-*s*-NIPAM) sample with X_{TEMPO} = 0.2 and X_{CL} = 0.03 system. Spherical nano-objects with diameters ranging from 30 to 50 nm were found. Those results agree with the DLS results and confirm our hypothesis concerning the formation of micellar nano-objects or nanogel particles containing TEMPO-rich hydrophobic domains when the amount of crosslinker is too low.

For higher amounts of crosslinker (i.e., 0.13), macroscopic gelation is observed (Table 1 and Figure 4)

TABLE 1 Macroscopic aspect of the P(TEMPO-*s*-NIPAM) hydrogels according to X_{TEMPO} and X_{CL}

X_{TEMPO} / X_{CL}	0	0.1	0.2	0.3	0.4
0.02	Liquid	Liquid	Liquid	Liquid	Liquid
0.03	Liquid	Liquid	Liquid	Liquid	Liquid
0.04	Gel	Liquid	Gel	Liquid	Liquid
0.05	Gel	Gel	Gel	Liquid	Liquid
0.13	Gel	Gel	Gel	Gel	Gel

Abbreviation: P(TEMPO-*s*-NIPAM), poly(2,2,6,6-tetramethylpiperidinoxy methacrylate-*statistical*-*N*-isopropylacrylamide).

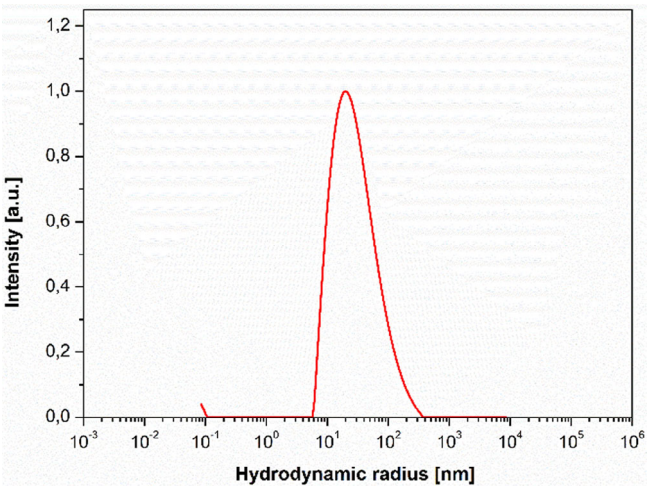

FIGURE 2 Size distribution histogram obtained by dynamic light scattering (DLS) on a poly(2,2,6,6-tetramethylpiperidinoxy methacrylate-*statistical*-*N*-isopropylacrylamide) P(TEMPO-*s*-NIPAM) solution with X_{TEMPO} = 0.2 and X_{CL} = 0.03 [Color figure can be viewed at wileyonlinelibrary.com]

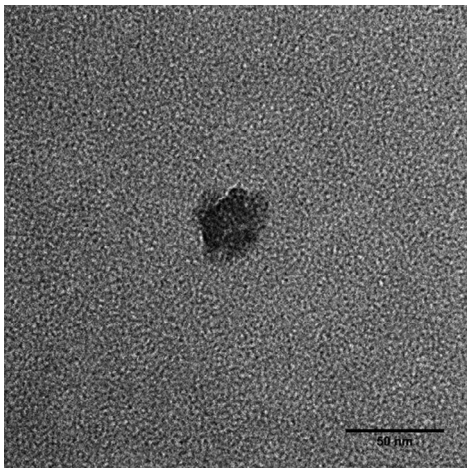

FIGURE 3 Cryogenic-transmission electron microscopy (cryo-TEM) image for a poly(2,2,6,6-tetramethylpiperidinoxy methacrylate-*statistical*-*N*-isopropylacrylamide) P(TEMPO-*s*-NIPAM) sample with $X_{TEMPO} = 0.2$ and $X_{CL} = 0.03$

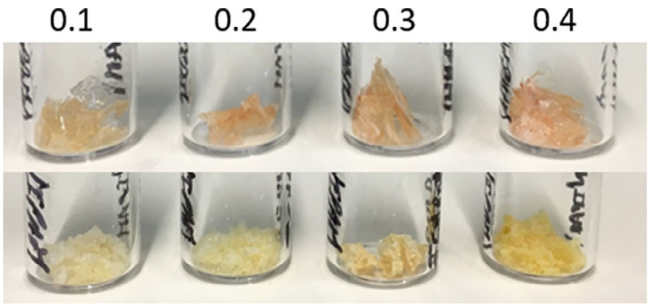

FIGURE 4 Library of the reduced poly (2,2,6,6-tetramethylpiperidinoxy methacrylate-*statistical*-*N*-isopropylacrylamide) P(TEMPO-*s*-NIPAM) (top) and oxidized P(TEMPO$^+$-*s*-NIPAM) (bottom) hydrogels with $X_{CL} = 0.13$ and different X_{TEMPO} (indicated on top) [Color figure can be viewed at wileyonlinelibrary.com]

meaning that the amount of crosslinker is sufficient to link together the micellar nano-objects or nanogel particles observed in Figures 2 and 3. Therefore, in the following of this article, the focus will be on the hydrogel-forming samples with $X_{CL} = 0.13$ and different $X_{TEMPO} = 0.1$, 0.2, 0.3, and 0.4 (Figure 4).

The oxidation of the P(TMPM-*s*-NIPAM) precursor into the P(TEMPO-*s*-NIPAM) hydrogel was macroscopically observed by the appearance of the orange color characteristic of nitroxide radicals (Figure 4). The oxidation yield of TMPM units into TEMPO ones was further determined by electron spin resonance (ESR). This method indicates an oxidation yield of about 99% and confirms that a high rate of oxidation has been reached for all the investigated hydrogels. As a typical example,

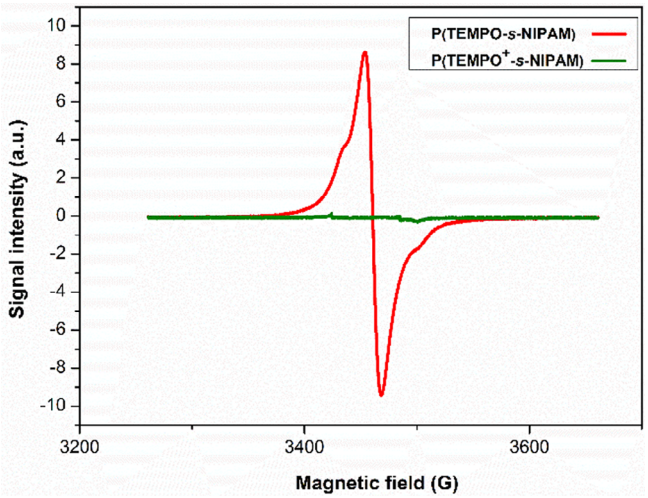

FIGURE 5 Electron spin resonance spectra of the poly (2,2,6,6-tetramethylpiperidinoxy methacrylate-*statistical*-*N*-isopropylacrylamide) P(TEMPO-*s*-NIPAM) (red line) and P(TEMPO$^+$-*s*-NIPAM) (green line) hydrogels ($X_{TEMPO} = 0.4$ and $X_{CL} = 0.13$) [Color figure can be viewed at wileyonlinelibrary.com]

Figure 5 (red line) shows for the P(TEMPO-*s*-NIPAM) hydrogel with $X_{TEMPO} = 0.4$ and $X_{CL} = 0.13$ a spin density of around 1.15×10^{-3} mol/g^1 with the typical signal shape for polymeric organic radicals, which confirms the presence of TEMPO radicals in this hydrogel.

Finally, the P(TEMPO-*s*-NIPAM) hydrogels were converted into P(TEMPO$^+$-*s*-NIPAM) ones by the chemical oxidation of the nitroxide radicals into oxoammonium cations using NaClO. This reaction can be visually monitored by the color change of the hydrogels from orange to yellow (Figure 4). ESR was also used to monitor this reaction. As a typical example, a spin ratio of about 10^{-6} mol/g^1 was measured for the P(TEMPO$^+$-*s*-NIPAM) hydrogel with $X_{TEMPO} = 0.4$ and $X_{CL} = 0.13$ and no characteristic signal belonging to radical species was clearly visualized (Figure 5, green line). From the spin density measurement, we deduce that only about 0.1% of the TEMPO units are not oxidized into TEMPO$^+$, which practically means that the conversion of the TEMPO units into TEMPO$^+$ ones is quantitative. Similar results have been obtained for all the investigated hydrogels.

3.2 | Mechanical properties

3.2.1 | Swelling studies

Swelling tests were performed on the P(TEMPO-*s*-NIPAM) hydrogels with $X_{CL} = 0.13$ (Figure 6). The swelling factor, defined as $[(W_s - W_d)/W_d]$, where W_s is the weight of the hydrogel in the swollen state at equilibrium

and W_d is the weight of the hydrogel in the dry state, was calculated. The equilibrium state was determined by regularly weighting the hydrogel during the swelling process until it reached a constant weight (typically after 24 hr).

However, the hydrogels were further equilibrated to reach a total time of 48 hr before measurement. P(TEMPO-*s*-NIPAM) hydrogels with X_{TEMPO} of 0.1, 0.2, and 0.3 display swelling factors around 140 (Figure 6a). For the hydrogel with $X_{TEMPO} = 0.4$, the swelling factor decreases by nearly a factor of two, which can be explained by the increase in hydrophobicity provided by the TEMPO units.

The swelling factors were significantly different for oxidized P(TEMPO$^+$-*s*-NIPAM) hydrogels with values around 85–90 for $X_{TEMPO} = 0.1$ and 0.2 (Figure 6b) and around 110 for X_{TEMPO} 0.3 and 0.4. In this case, the value of the swelling factor increases with the content in TEMPO$^+$ groups which is expected since TEMPO$^+$ groups are hydrophilic in contrast to hydrophobic TEMPO groups. The swelling factor values are smaller for the P(TEMPO$^+$-*s*-NIPAM) hydrogels compared to the P(TEMPO-*s*-NIPAM) ones in agreement with our previous studies on P(TEMPO-*s*-OEGMA) and P(TEMPO$^+$-*s*-OEGMA) hydrogels.[25,26]

The temperature-dependent swelling profiles of the P(TEMPO-*s*-NIPAM) hydrogels with varying amounts of TEMPO units and X_{CL} equal to 0.13 are illustrated in Figure 7. As temperature increases, swelling decreases until 80°C, when all gels totally collapsed. The swelling factors decrease significantly between 20 and 25°C for all the investigated P(TEMPO-*s*-NIPAM) hydrogels in agreement with the desolvation of NIPAM units and in line with the milky macroscopic aspect of the hydrogels. This occurs at temperatures a bit lower than the reported LCST of PNIPAM (32°C). This observation is expected since the presence of hydrophobic TEMPO units should shift the LCST to lower temperatures.[28] On the other hand, we have previously demonstrated that solubility of TEMPO units increases as temperature increases.[26] This effect would explain why a complete collapse of the P(TEMPO-*s*-NIPAM) hydrogels is not observed above the LCST of NIPAM units but rather a slow desolvation of the hydrogels as temperature increases (Figure 7).

As far as P(TEMPO$^+$-*s*-NIPAM) hydrogels are concerned, the swelling factors are found to be constant whatever the temperature and the amount of X_{TEMPO+}. Therefore, it seems that the hydrophilic character of

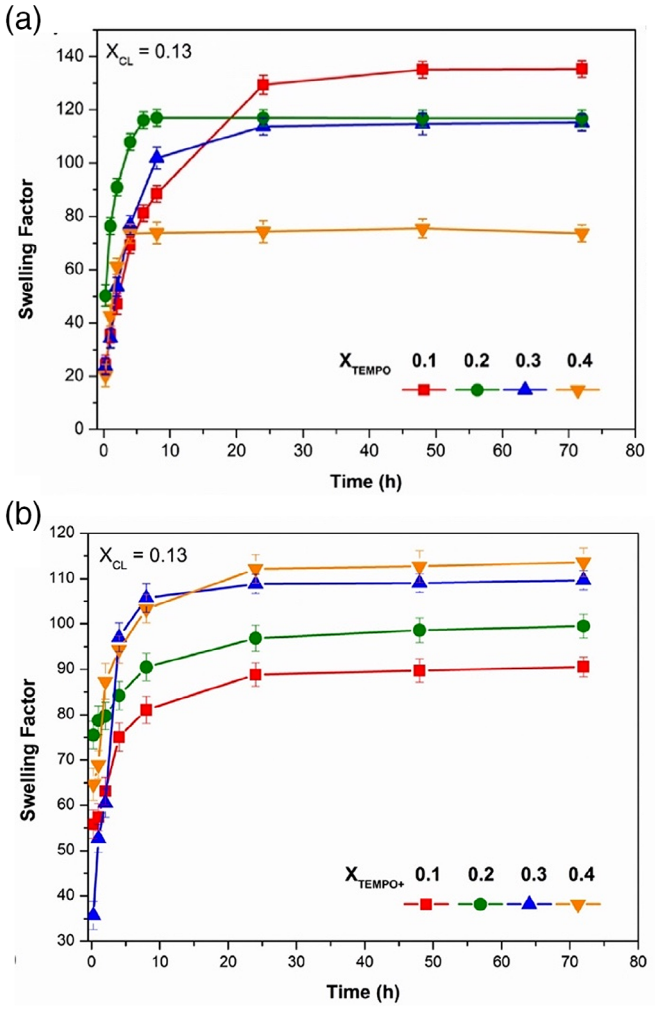

FIGURE 6 Kinetic swelling study of (a) poly (2,2,6,6-tetramethylpiperidinoxy methacrylate-*statistical*-*N*-isopropylacrylamide) P(TEMPO-*s*-NIPAM) and (b) P(TEMPO$^+$-*s*-NIPAM) hydrogels with varying X_{TEMPO} (X_{CL} fixed to 0.13, error bars represent average swelling ratio ± *SD*, where $n = 3$) [Color figure can be viewed at wileyonlinelibrary.com]

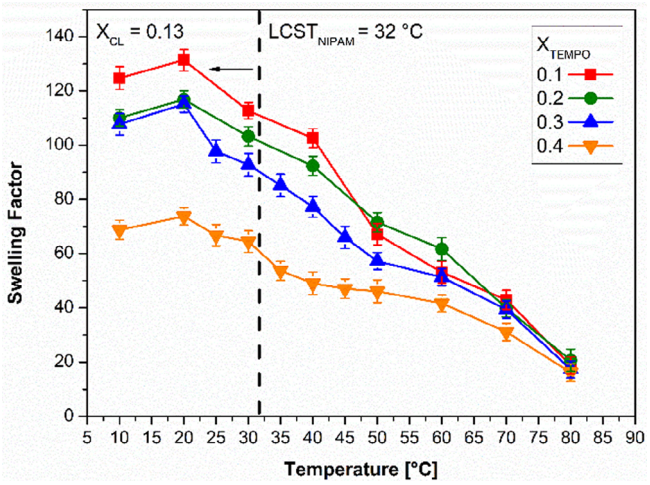

FIGURE 7 Temperature-dependent swelling profiles of poly (2,2,6,6-tetramethylpiperidinoxy methacrylate-*statistical*-*N*-isopropylacrylamide) P(TEMPO-*s*-NIPAM) hydrogels for different X_{TEMPO} and $X_{CL} = 0.13$ (error bars represent average swelling ratio ± *SD*, where $n = 3$) [Color figure can be viewed at wileyonlinelibrary.com]

TEMPO$^+$ units is totally overwhelming the effect of the LCST of PNIPAM which has not been observed for the investigated samples. Indeed, all the P(TEMPO-*s*-NIPAM) hydrogels remains optically clear whatever the temperature meaning that the LCST of PNIPAM is not reached in our experimental window of parameters.

3.2.2 | Rheological properties

The viscoelastic properties of the P(TEMPO-*s*-NIPAM) hydrogels were investigated by rotational rheometry. The viscoelastic response was measured as a function of the oscillation frequency for the different X_{TEMPO} values and for $X_{CL} = 0.13$. As shown in Figure 8, the storage modulus (G') is constant in the whole experimental frequency range, confirming the formation of a gel. By adding more TEMPO units in the hydrogel, G' increases. Since these units are insoluble in water, we hypothesize that TEMPO groups aggregate into hydrophobic domains that could be at the origin of the nanostructures observed by cryo-TEM (Figure 3). As suggested before, those hydrophobic domains could play the role of additional physical crosslinks to the chemical crosslinks provided by the DEGDA units, which nicely explains the increase of the elastic modulus of our hydrogels with increasing X_{TEMPO}.

Regarding the oxidized P(TEMPO$^+$-*s*-NIPAM) hydrogels, frequency sweeps were also performed that confirm gel formation (Figure 8).

While comparing the rheological properties of the P(TEMPO-*s*-NIPAM) and P(TEMPO$^+$-*s*-NIPAM) hydrogels, we observe that the oxidized P(TEMPO$^+$-*s*-NIPAM) hydrogels display higher moduli than the P(TEMPO-*s*-NIPAM) ones although the physical crosslinks due to hydrophobic TEMPO domains disappear upon oxidation of the nitroxide radicals into soluble oxoammonium cations. We attribute the higher G' in P(TEMPO$^+$-*s*-NIPAM) hydrogels to a stiffening of the polymer network resulting from electrostatic repulsions among positively charged TEMPO$^+$ units. This is consistent with the observation of the swelling behavior discussed above. The evolution of the storage modulus as a function of temperature is presented in Figure S2 and is fully consistent with the temperature-dependent swelling data (Figure 7), that is, G' decreases with temperature for P(TEMPO-*s*-NIPAM) hydrogels and is constant for P(TEMPO$^+$-*s*-NIPAM) hydrogels in the investigated temperature range.

In order to investigate the reversible behavior of our hydrogels, strain sweeps have been performed from low to high strain amplitude and then from high to low strain. The results are shown in Figure 9 for the P(TEMPO-*s*-NIPAM) hydrogels with $X_{TEMPO} = 0.1$ (lowest amount) and 0.4 (highest amount) and $X_{CL} = 0.13$.

For both samples, hysteresis is observed, which can be seen as a signature of reversible association operating in our hydrogels. While the network structure is partially broken at high strain in order to allow the sample to deform, the network is reformed when coming back to low strain amplitude. This behavior can be explained by the hypothesized structure of our hydrogels previously

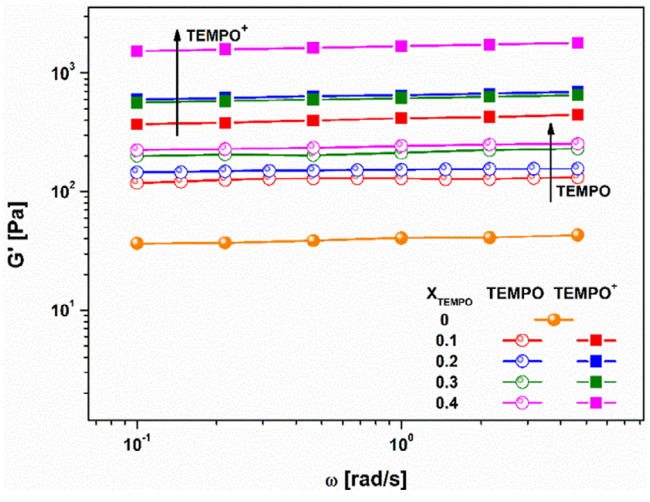

FIGURE 8 Frequency sweep plots of storage versus frequency for poly(2,2,6,6-tetramethylpiperidinoxy methacrylate-*statistical*-*N*-isopropylacrylamide) P(TEMPO-*s*-NIPAM) and P(TEMPO$^+$-*s*-NIPAM) hydrogels with varying X_{TEMPO} and $X_{CL} = 0.13$ [Color figure can be viewed at wileyonlinelibrary.com]

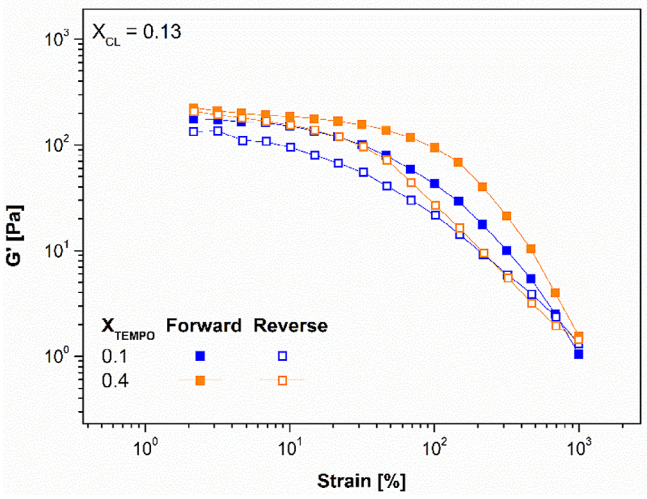

FIGURE 9 Storage modulus of the poly (2,2,6,6-tetramethylpiperidinoxy methacrylate-*statistical*-*N*-isopropylacrylamide) P(TEMPO-*s*-NIPAM) hydrogels with $X_{CL} = 0.13$ and $X_{TEMPO} = 0.1$ (blue) or 0.4 (yellow), from low to high (filled symbols) or high to low (empty symbols) amplitude of deformation [Color figure can be viewed at wileyonlinelibrary.com]

described in this contribution. Indeed, our hydrogels are believed to consist of micellar/nanogel particles containing a TEMPO-rich core that are usually linked together by chemical crosslinks. However, a significant amount of nano-objects could be trapped in the network structure through reversible association of the TEMPO groups, but without being covalently linked to this network. Therefore, upon deformation, those ones could dissociate from the covalent network compromising its integrity. Nevertheless, this behavior is reversible allowing the network to reform when deformation is stopped.

The strain sweep experiment carried out on oxidized P(TEMPO$^+$-*s*-NIPAM) hydrogels basically show the same behavior (Figure S3), confirming our hypothesis about the structure of the hydrogel. In sharp contrast, the reference gel containing only NIPAM and DEGDA (and thus no TEMPO) keeps its integrity upon high deformation (Figure S4). However, in order to enter its nonlinear regime of deformation, covalent bonds have to break and the sample does not recover its initial state with lowering the strain amplitude. In this case, no micellar/nanogel substructure is present and only chemical crosslinking points are responsible for network formation.

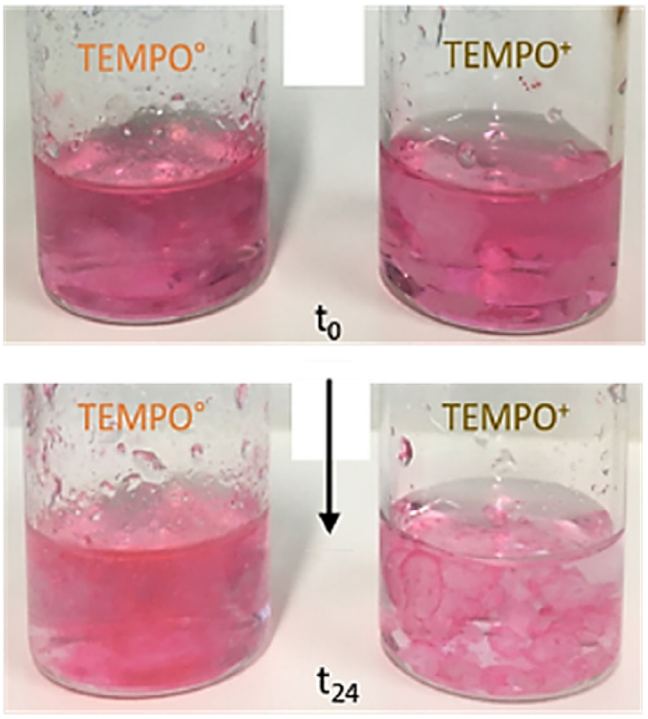

FIGURE 10 Encapsulation of Eosin B via two strategies: electrostatic interaction (for 2,2,6,6-tetramethylpiperidinoxy methacrylate (TEMPO$^+$) containing hydrogels and entrapping by swelling for TEMPO containing hydrogels (hydrogels with $X_{TEMPO} = 0.4$ and $X_{CL} = 0.13$) [Color figure can be viewed at wileyonlinelibrary.com]

3.3 | Encapsulation properties

In order to demonstrate the encapsulation abilities of our hydrogels, we have designed a proof-of-concept experiment taking opportunity of the presence of positively charged units in the oxidized P(TEMPO$^+$-*s*-NIPAM) hydrogels to encapsulate a negatively charged model molecule, namely Eosin B. Eosin B was selected since it can be easily visually followed by its pink-red color. In a first experiment, water containing Eosin B at a concentration of 0.012 g/L was used to realize the equilibrium swelling of either the P(TEMPO-*s*-NIPAM) or the P(TEMPO$^+$-*s*-NIPAM) hydrogels. As macroscopically observed in Figure 10, both P(TEMPO-*s*-NIPAM) and the P(TEMPO$^+$-*s*-NIPAM) (both prepared from the network with $X_{TEMPO} = 0.4$ and $X_{CL} = 0.13$) do form hydrogels with encapsulated Eosin B. Nevertheless, the supernatant from the hydrogel prepared from the P(TEMPO$^+$-*s*-NIPAM) (Figure 10) seems to be colorless while the one from the P(TEMPO-*s*-NIPAM) sample (Figure 10) still presents the same characteristic pink color as the one of the starting Eosin B solution at t_0. This preliminary observation suggests that ionic interactions are formed between P(TEMPO$^+$-*s*-NIPAM) and Eosin B that could explain the sequestration of Eosin B molecules into the hydrogel. In the case of the P(TEMPO-*s*-NIPAM) hydrogel, Eosin B seems to be homogeneously dispersed in the hydrogel and in the supernatant.

This observation was confirmed by ultraviolet–visible measurements realized on the supernatant after

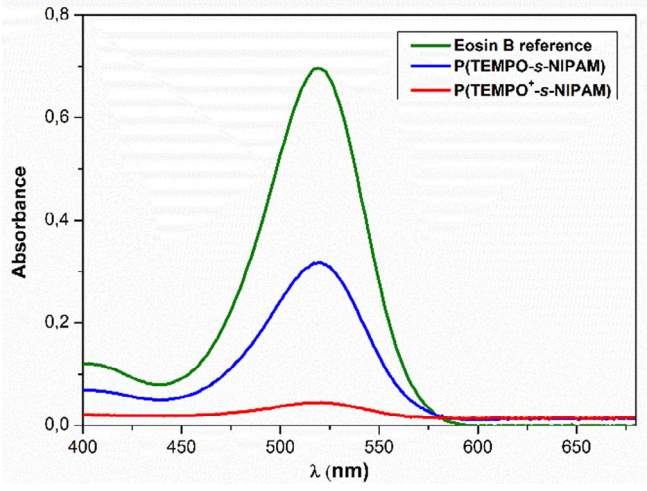

FIGURE 11 Ultraviolet–visible spectra of the supernatant of poly(2,2,6,6-tetramethylpiperidinoxy methacrylate-*statistical*-*N*-isopropylacrylamide) P(TEMPO-*s*-NIPAM) (blue line) and P(TEMPO$^+$-*s*-NIPAM) (red line) hydrogels after equilibrium swelling in Eosin B solution (hydrogels prepared from the networks with $X_{TEMPO} = 0.4$ and $X_{CL} = 0.13$) [Color figure can be viewed at wileyonlinelibrary.com]

equilibration. As observed in Figure 11, the characteristic absorption peak of Eosin B at 514 nm is still observed in the supernatant of the P(TEMPO-*s*-NIPAM) hydrogel (an encapsulation ability ~13% has been determined by using Beer–Lambert law) while it is not observed in the supernatant of the P($TEMPO^+$-*s*-NIPAM) sample (encapsulation ability ~99%) confirming strong electrostatic interactions between the charged $TEMPO^+$ units and negatively charged Eosin B molecules in the case of the P($TEMPO^+$-*s*-NIPAM) hydrogel.

4 | CONCLUSIONS

In this study, we have obtained polymer-based hydrogels responding either to redox or temperature stimuli by introducing NIPAM and TEMPO comonomers into a polymer network. The LCST behavior of PNIPAM has been used to induce deswelling of the hydrogels with increasing temperature while the oxidation of the nitroxide radicals of TEMPO into oxoammonium cations has allowed the transformation of hydrophobic TEMPO into hydrophilic $TEMPO^+$. The application of the redox and temperature stimuli has triggered important change in the mechanical behavior of the hydrogels as monitored by the determination of swelling factors and of rheological properties. Notably, it was observed that TEMPO units aggregate into hydrophobic nanodomains acting as supplementary physical crosslinking nodes in addition to the chemical crosslinking points provided by the difunctional crosslinking agent. Upon oxidation, those nanodomains are suppressed in favor of positively charged $TEMPO^+$ units conferring a polyelectrolyte character. In addition, we have shown that the thermoresponsive properties are influenced by the redox state of the TEMPO units. Indeed, hydrophobic TEMPO units tend to lower the LCST of PNIPAM while hydrophilic $TEMPO^+$ groups seem to shift the LCST to higher temperatures or even suppress it.

Interestingly, we have also linked the microstructure of the polymer network to the macroscopic properties of the hydrogels. In this respect, the large difference in reactivity ratios between the comonomers leads to the formation of TEMPO-rich segments in the early stages of the polymerization that further aggregate into micellar nano-objects or nanogel particles. If too low amounts of bifunctional crosslinker are added, those nano-objects are not linked together in the later stage of the polymerization, leading to viscous solutions rather than macroscopic hydrogels. Those nanoparticles have indeed been observed by DLS and cryo-TEM. If the concentration of bifunctional crosslinker is high enough, the nano-objects are eventually linked together leading to a macroscopic hydrogel. The accordingly obtained hydrogels are however rather mechanically weak and can be reversibly disrupted through strain sweep experiments. This suggests that a fraction of nano-objects is simply entrapped in the network and can be disentangled when a mechanical deformation is applied.

To end, the encapsulation abilities of those hydrogels have been tested by encapsulating a negatively charged guest molecule through electrostatic interactions with the positively charged $TEMPO^+$ units. These novel stimuli-responsive hydrogels can be very relevant for many applications in material science and biotechnology.

ACKNOWLEDGMENTS

M. K. is grateful to the International Relations Office (ADRI) of UClouvain and to the Concerted Research Action BATTAB (14/19-057) for financing her PhD. J. F. G. is grateful to the Fondation Louvain through the 2018 Marcel de Merre Price for Nanotechnologies for financing this research. U. S. S. is grateful for support via the RIS3 Innovation Center CEEC Jena. E. V. R. is research associate of the FRS-FNRS.

ORCID

Ulrich S. Schubert https://orcid.org/0000-0001-8572-8153

Evelyne Van Ruymbeke https://orcid.org/0000-0001-7633-0194

Jean-François Gohy https://orcid.org/0000-0003-4169-1883

REFERENCES

[1] L. D. Zarzar, J. Aizenberg, *Acc. Chem. Res.* **2014**, *47*, 530.
[2] H. Huang, X. Qi, Y. Chen, Z. Wu, *Saudi Pharm. J.* **2019**, *27*, 990.
[3] S. H. Park, H. S. Shin, S. N. Park, *Carbohydr. Polym.* **2018**, *200*, 341.
[4] C. Lv, X. C. Sun, H. Xia, Y. H. Yu, G. Wang, X. W. Cao, S. X. Li, Y. S. Wang, Q. D. Chen, Y. de Yu, H. B. Sun, *Sens. Actuat. B Chem.* **2018**, *259*, 736.
[5] L. Li, J. M. Scheiger, P. A. Levkin, *Adv. Mater.* **2019**, *31*, 1.
[6] H. Jiang, Z. Qin, Y. Zheng, L. Liu, X. Wang, *Small* **2019**, *15*, 1.
[7] J. Kolosnjaj-Tabi, L. Gibot, I. Fourquaux, M. Golzio, M. P. Rols, *Adv. Drug Deliv. Rev.* **2019**, *138*, 56.
[8] T. Xiang, T. Lu, W. F. Zhao, C. S. Zhao, *Langmuir* **2019**, *35*, 1146.
[9] D. Singh, D. Kuckling, V. Koul, V. Choudhary, H. J. Adler, A. K. Dinda, *Eur. Polym. J.* **2008**, *44*, 2962.
[10] J. Kopecek, *Nature* **2002**, *417*, 388.
[11] G. Li, I. Dobryden, E. J. Salazar-Sandoval, M. Johansson, P. M. Claesson, *Soft Matter* **2019**, *15*, 7704.
[12] E. Isikci Koca, G. Bozdag, G. Cayli, D. Kazan, P. Cakir Hatir, *J. Appl. Polym. Sci.* **2019**, *48861*, 1.
[13] M. A. Haq, Y. Su, D. Wang, *Mater. Sci. Eng. C* **2017**, *70*, 842.

[14] P. Li, X. Hou, L. Qu, X. Dai, C. Zhang, *Polymers (Basel).* **2018**, *10*, 2.
[15] B. Strachota, A. Strachota, M. Šlouf, J. Brus, V. Cimrová, *Soft Matter* **2019**, *15*, 752.
[16] M. Cao, Y. Wang, X. Hu, H. Gong, R. Li, H. Cox, J. Zhang, T. A. Waigh, H. Xu, J. R. Lu, *Biomacromolecules* **2019**, *20*, 3601.
[17] M. V. Martinez, M. Molina, C. A. Barbero, *J. Phys. Chem. B* **2018**, *122*, 9038.
[18] S. Shekhar, M. Mukherjee, A. K. Sen, *Adv. Mater. Res.* **2012**, *1*, 269.
[19] X. Feng, K. Zhang, P. Chen, X. Sui, M. A. Hempenius, B. Liedberg, G. J. Vancso, *Macromol. Rapid Commun.* **2016**, *37*, 1939.
[20] M. Hrubý, S. K. Filippov, P. Štěpánek, *Eur. Polym. J.* **2015**, *65*, 82.
[21] X. Sui, X. Feng, M. A. Hempenius, G. J. Vancso, *J. Mater. Chem. B* **2013**, *1*, 1658.
[22] C. J. Pérez-Martínez, S. D. Morales Chávez, T. del Castillo-Castro, T. E. Lara Ceniceros, M. M. Castillo-Ortega, D. E. Rodríguez-Félix, J. C. Gálvez Ruiz, *React. Funct. Polym.* **2016**, *100*, 12.
[23] P. L. Bragd, A. C. Besemer, H. van Bekkum, *J. Mol. Catal. A Chem.* **2001**, *170*, 35.
[24] N. Hiroyuki, O. Kenichi, *Science* **2008**, *319*, 737.
[25] M. Khodeir, B. Ernould, J. Brassinne, S. Ghiassinejad, H. Jia, S. Antoun, C. Friebe, U. Schubert, S. Kochovski, Z. Lu, Y. Ruymbeke, E. van Gohy, *Soft Matter* **2019**, *15*, 6418.
[26] M. Khodeir, S. Antoun, E. van Ruymbeke, J. Gohy, *Macromol. Chem. Phys.* **2020**, *1900550*, 1.
[27] J. Virtanen, H. Tenhu, *J. Polym. Sci. Part A: Polym. Chem.* **2001**, *39*, 3716.
[28] G. Gürdağ, B. Kurtuluş, *Ind. Eng. Chem. Res.* **2010**, *49*, 12675.

SUPPORTING INFORMATION

Additional supporting information may be found online in the Supporting Information section at the end of this article.

How to cite this article: Khodeir M, Jia H, Antoun S, et al. Synthesis and characterization of hydrogels containing redox-responsive 2,2,6,6-tetramethylpiperidinyloxy methacrylate and thermoresponsive *N*-isopropylacrylamide. *J Polym Sci*. 2020;1–11. https://doi.org/10.1002/pol.20200172